Molecular ferroelectrics: where electronics meet biology

Jiangyu Li,*[a] Yuanming Liu,[a] Yanhang Zhang,[b] Hong-Ling Cai[c] and Ren-Gen Xiong[c]

In the last several years, we have witnessed significant advances in molecular ferroelectrics, with the ferroelectric properties of molecular crystals approaching those of barium titanate. In addition, ferroelectricity has been observed in biological systems, filling an important missing link in bioelectric phenomena. In this perspective, we will present short historical notes on ferroelectrics, followed by an overview of the fundamentals of ferroelectricity. The latest developments in molecular ferroelectrics and biological ferroelectricity will then be highlighted, and their implications and potential applications will be discussed. We close by noting molecular ferroelectric as an exciting frontier between electronics and biology, and a number of challenges ahead are also described.

1. Introduction

When a dielectric is placed in an electric field, it becomes polarized – positive and negative charges are separated, producing a dipole with dipole moment given by the product of the charges and their separation distance. The polarization is then defined as the dipole moment per unit volume. Simultaneously, the dielectric experiences an electrostrictive strain, which is quadratic to the polarization, though the electrostriction is usually negligibly small and bears no practical significance. However, if the dielectric is not central-symmetric, a relatively large piezoelectric strain proportional to the electric field is also possible. Among 21 crystalline classes without a symmetry center, 20 of them are piezoelectric, within which 10 of them possess a unique polar axis that is spontaneously polarized.[1] These 10 polar classes are referred to as pyroelectric, whose spontaneous polarization varies with temperature. If such spontaneous polarization can be reversed by an external electric field, then the pyroelectric is also ferroelectric, and ferroelectricity refers to the switchability of spontaneous polarization, which usually results in a hysteresis loop between polarization and the electric field. The relationships among dielectric, piezoelectric, pyroelectric and ferroelectric materials are shown in Fig. 1(a), and a schematics of polarization switching in ferroelectrics are shown in Fig. 1(b).

Ferroelectrics are fascinating materials with versatile properties and important applications in data storage, sensing, actuation,
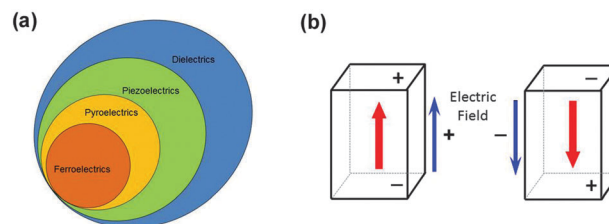
Fig. 1 (a) The relationships among dielectric, piezoelectric, pyroelectric and ferroelectric materials; (b) bipolar state of ferroelectrics that can be switched by external electric field.

energy harvesting and electro-optic devices, among others.[2] Recently, we have witnessed exciting progress in molecular ferroelectrics and biological ferroelectricity. For example, molecular ferroelectrics with properties comparable to those of perovskite oxides have been synthesized,[3,4] and ferroelectricity in biological materials and systems have been observed.[5–8] In this perspective, we will present short historical notes on ferroelectrics, followed by an overview of the fundamentals of ferroelectricity. The latest developments in molecular ferroelectrics and biological ferroelectricity will then be highlighted, and their implications and potential applications will be discussed. This is not intended to be a comprehensive review of state of the art; rather it reflects our personal reflections and perspective on the field.

2. Historical notes

The history of ferroelectrics can be traced back to 1655, when Rochelle salt was first separated by Elie Seignette in France, though pyroelectricity has been known since ancient times. But it was not until more than 200 years later that the piezoelectricity

[a] Department of Mechanical Engineering, University of Washington, Seattle, WA 98195-2600, USA. E-mail: jjli@uw.edu

[b] Department of Mechanical Engineering, and Department of Biomedical Engineering, Boston University, Boston, MA 02215, USA

[c] Ordered Matter Science Research Centre, Southeast University, Nanjing 211189, P. R. China

of Rochelle salt was established by Curie's brother in 1880.[9] It took another 40 years before the hysteretic nature of Rochelle salt polarization was demonstrated by Joseph Valasek in 1920,[10] who coined the term 'ferroelectric' to reflect its analogies with ferromagnetism. For a while, Rochelle salt was the only known ferroelectric material, until ferroelectricity was discovered in KH_2PO_4 (KDP) by Busch and Scherer in 1935.[11] The breakthrough came in the 1940s during the Second World War, when barium titanate (BTO) of a simple perovskite structure was synthesized, with its ferroelectricity demonstrated by von Hippel in 1945.[12] Piezoelectric transducers were developed, and many new ferroelectric perovskite oxides were synthesized. The most notable one was lead zirconate titanate (PZT), first reported by Shirane and coworkers in 1952,[13] and its ferroelectricity was demonstrated by Sawaguchi in 1953.[14] Today, PZT remains the most widely used ferroelectric materials, though its lead content is a major environmental concern, and there are considerable efforts to search for its lead-free alternatives.

While ferroelectricity was first observed in Rochelle salt, a molecular crystal, the rapid advances of the field only occurred after the development of ionic ferroelectrics such as BTO and PZT. These perovskite oxides exhibit superior ferroelectric properties, orders of magnitude higher than those of molecular crystals, though they are rigid and heavyweight, contain toxic lead, and require high temperature processing. In 1969, strong piezoelectricity was discovered in polyvinylidene fluoride (PVDF) by Kawai,[15] and its ferroelectricity was subsequently verified,[16,17] with spontaneous polarization measured around 8 $\mu C\ cm^{-2}$, on the same order of barium titanate. This opens the door for practical applications of PVDF and its copolymers, which are soft and flexible, lightweight, lead free, processed at relatively low temperature, and biocompatible. Today, PVDF and its copolymer are the most widely used ferroelectric polymers, though a number of exciting new molecular ferroelectrics have been developed in recent years, with properties approaching those of BTO, which has motivated this perspective.

Another exciting advance closely related to molecular ferroelectrics is the recent observation of biological ferroelectricity. Piezoelectricity in biological systems was noticed first in 1940. When wool fibers are rubbed together the sign of the electric charges produced by friction, the so-called triboelectric charges,

depends on the type of rubbing, and A. J. P. Martin attributed such a phenomenon to pyroelectric and piezoelectric effects.[18] Former Soviet Union physicist Bazhenov and his colleagues observed piezoelectricity in wood in early 1950s,[19,20] and Eiichi Fukada and Yasuda Iwao published a landmark paper in 1957, reporting piezoelectricity in bone.[21] Many biological tissues were proven piezoelectric afterward, leading to speculation that piezoelectricity is a fundamental property of biological tissues.[22] For example, it was suggested that piezoelectricity played an important role in bone growth and remodeling.[23] Not long after the discovery of biological piezoelectricity, pyroelectricity was reported in bone and tendon by Sidney Lang in 1966,[24] and subsequently in many other biological systems as well,[25] leading to speculation of the existence of biological ferroelectricity,[26] as one would expect from Fig. 1(a). There are actually fascinating theories developed on biological ferroelectricity for ion channels, hypothesizing conformational transitions in voltage-dependent ion channels in terms of transitions from a ferroelectric state to a superionically conducting state.[27] These theories were motivated by a number of experimental observations in ion channels, and a relation between ferroelectricity, liquid crystals and nervous and muscular impulses was predicted by von Hippel. Nevertheless, no direct experimental evidence has been presented until very recently, and it took almost 50 years for biological ferroelectricity to be demonstrated experimentally since Lang's discovery of biological pyroelectricity. The observations of ferroelectricity in biological systems fills an important missing link in not only bioelectric phenomena, but also molecular ferroelectrics, which we believe stand right between electronics and biology.

3. Fundamentals of ferroelectricity

There are a number of excellent monographs on ferroelectricity, and the readers can refer to the classical book of Lines and Glass[2] for more information. The defining characteristics of ferroelectrics is the possession of spontaneous polarization P_s that can be switched by an external electric field E, resulting in a polarization-field hysteresis loop, as shown in Fig. 2(a), from which the spontaneous polarization P_s, remnant polarization P_r, and coercive field E_c can be identified. Such spontaneous polarization also provides an internal bias to the ferroelectric,
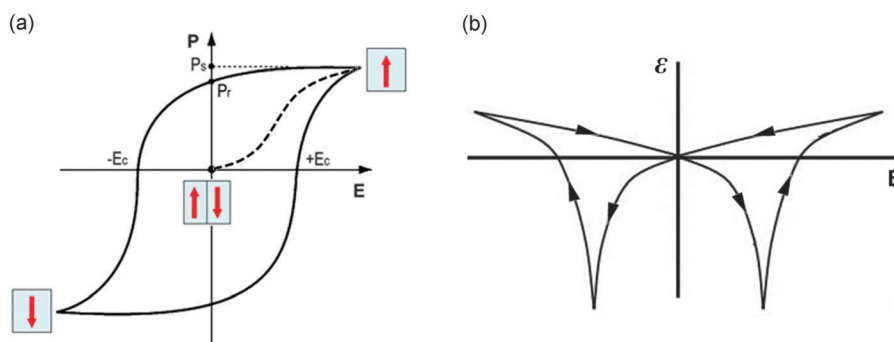

Fig. 2 Ferroelectric hysteresis (a) and butterfly loops (b).

resulting in the loss of central-symmetry and a large piezo-electric strain ε,[2]

$$\varepsilon = Q(P_s + \chi E)^2 \approx QP_s^2 + 2Q\chi P_s E, \tag{1}$$

where the first term is quadratic electrostrictive strain, and the second term is linear piezoelectric strain; Q and χ are electrostrictive coefficient and dielectric susceptibility, respectively. Since Q does not vary much among different materials,[2] eqn (1) suggests that large spontaneous polarization and dielectric susceptibility can lead to a large piezoelectric effect, which is consistent with experimental observations, and explains why a good ferroelectric is usually a good piezoelectric as well. Furthermore, as electric field and spontaneous polarization are both reversed, the field induced strain does not change sign, which is evident from eqn (1), resulting in a characteristic butterfly loop between the strain and electric field, as shown in Fig. 2(b), which is symmetric with respect to the axis of zero field.

A uniform distribution of polarization is usually energetically disfavored due to the large depolarization field associated with it, and ferroelectrics often form complicated microscopic domain patterns with distinct polarization distribution to minimize the electrostatic energy. Indeed, the macroscopic ferroelectric hysteresis loop does reflect the evolution of microscopic domain patterns under an external electric field, as shown schematically in Fig. 2(a). In addition, the spontaneous polarization decreases with increased temperature T, from which the pyroelectric current can be measured, with pyroelectric coefficient p defined as[2]

$$p = \frac{dP_s}{dT}, \tag{2}$$

whose sign depends on the direction of the polar axis. There exists a Curie temperature T_c, upon which the structural phase transition occurs and the material becomes non-polar, and the spontaneous polarization vanishes. The microscopic mechanism of phase transition can be either order–disorder or displacive type, and the dielectric constant κ often shows an anomaly approaching phase transition, as described by the Curie–Weiss law,[2]

$$\kappa/\kappa_0 = \frac{C}{T - T_0}, \tag{3}$$

where κ_0 is the permittivity of vacuum, C is the Curie constant, and T_0 is the Curie–Weiss temperature. Many molecular ferroelectrics show order–disorder transition with C on the order of

10^3 K while oxide ferroelectrics are usually displacive type with C on the order of 10^5 K. Some ferroelectrics show mixed characteristics of order–disorder and displacive transition as well. Depending on whether the spontaneous polarization changes continuously or discontinuously at the Curie point, the phase transition can also be classified as second or first order.

Because of the nonlinear relationship between the polarization and electric field in ferroelectrics, they also show a notable electro-optic effect and possess nonlinear optic coefficients. In particular, it can be shown that the second order nonlinear optic coefficient $\chi^{(2)}$ scales with spontaneous polarization,[28]

$$\chi^{(2)} \propto P_s, \tag{4}$$

which has been confirmed by experimental data.[28] This suggests that ferroelectrics with large spontaneous polarization would have large second harmonic generation (SHG) as well.

There are a number of methods to identify possible ferroelectricity in a material. The ferroelectric phase transition can be studied by differential scanning calorimetry (DSC) and X-ray diffraction (XRD). The transition from a high temperature non-polar phase to a low temperature polar structure can also be captured by the emergence of SHG at the Curie point, based on eqn (4), and a dielectric anomaly in the form of eqn (3) is also a good indication of ferroelectric phase transition. Nevertheless, a hysteresis loop measured by the Sawyer–Tower circuit is the most straightforward demonstration of ferroelectricity, and is considered as the signature of polarization switching. Measurement of the pyroelectric current by dynamic temperature change is another method,

$$i = \frac{A dP_s}{dt} = pA\frac{dT}{dt}, \tag{5}$$

where A is the area of surface electrode, and the reversal of pyroelectric current is a good sign of polarization switching. All these techniques have been employed to study molecular ferroelectrics.

The macroscopic hysteresis measurement might not always be possible, especially for materials with large coercive field or leakage current, or for materials that are difficult to grow into a large sample. The emergence of piezoresponse force microscopy (PFM) offers a powerful tool to probe local piezoelectricity and ferroelectricity at the nanoscale.[29] The principle of PFM is shown schematically in Fig. 3(a). An AC voltage is applied to the
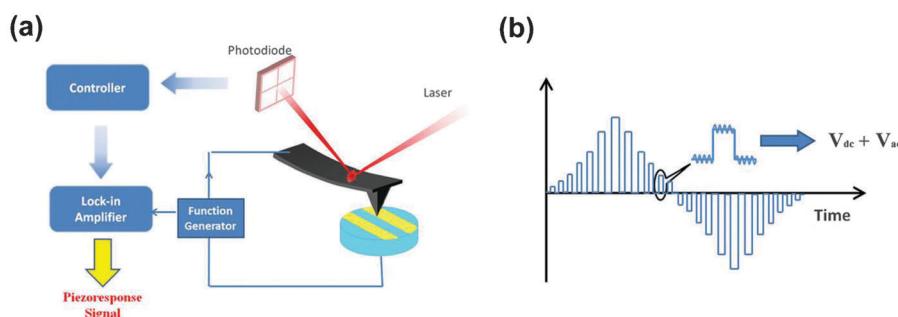

Fig. 3 Schematics of PFM (a) and switching PFM (b).

specimen by the conductive scanning probe microscopy (SPM) tip, and if the material is piezoelectric, local piezoelectric vibration will be excited, which is measured by the laser diode. The amplitude of the PFM vibration reflects the magnitude of the piezoelectric coefficient, while the PFM phase reflects the direction of the polar axis. Thus by scanning over the sample, mappings of PFM phase and amplitude will be obtained, representing the underlying ferroelectric domain structure. Furthermore, by imposing the AC voltage on top of a sequence of DC voltage, as shown in Fig. 3(b), wherein the DC voltage is used to switch the spontaneous polarization and AC voltage is used to excite the piezoelectric vibration for measurement, a characteristic phase–voltage hysteresis loop and amplitude–voltage butterfly loops can also be obtained. It is worth emphasizing that the PFM hysteresis loop, while indicating reversal of the polar axis through the switching of PFM phase, does not measure the polarization as in the classical Sawyer–Tower circuit, and thus no spontaneous polarization can be obtained directly from PFM measurement. Nevertheless, the existence of PFM phase contrast and the reversal of a PFM phase under external voltage is a good indication of ferroelectricity, and this turns out to be instrumental in recent probing of molecular and biological ferroelectrics.

4. Recent developments of molecular ferroelectrics

Microscopically, ferroelectricity can arise from either displacive or order–disorder transition, and both types have been explored in molecular systems. Although relative ionic displacement in perovskite oxides has resulted in large spontaneous polarization and excellent piezoelectric and ferroelectric properties in BTO and PZT, such a mechanism is less successful in molecular systems. One recent example is 4-(cyanomethyl) anilinium perchlorate (CMAP), which recorded a hysteresis loop with spontaneous polarization of 0.75 μC cm^{-2}, slightly smaller than those estimated from DSC (0.99 μC cm^{-2}).[28] Detailed structure analysis suggested that NH_3^+ and ClO_4^- ions are displaced upon phase transition, resulting in a separation of positive and negative charges with a dipole moment of 1.49 Debye, from which the spontaneous polarization is calculated to be 1.06 μC cm^{-2}, in good agreement with DSC and heat capacity measurements. It is interesting to note that the dipole moment of CMAP is comparable to that of BTO (3.18 Debye), yet the spontaneous polarization is much smaller, because its molecular volume is much larger. This is indeed one of the limiting factors for displacive molecular ferroelectrics. In the following, we summarize four strategies in searching for high performance molecular ferroelectrics that have been explored recently. More information can be found in recent comprehensive reviews,[30,31] though a number of exciting advances have been made since then, which we will highlight.

The first strategy is to utilize the oppositely charged electron donor (D) and acceptor (A) in the charge transfer complex, especially in multi-component systems, to create a polar structure.
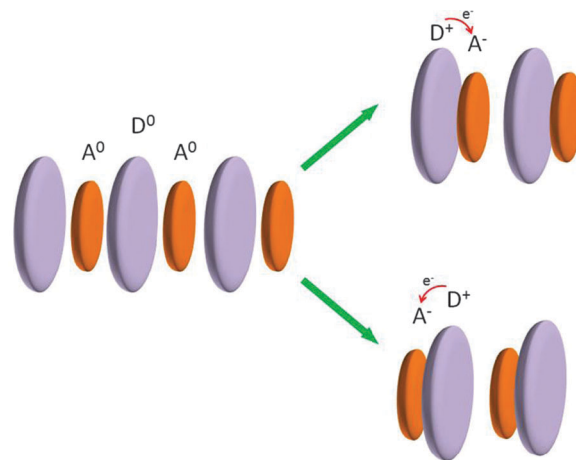

Fig. 4 Schematics of neutral-to-ionic transition in the charge transfer complex.

The idea is to explore the molecular chain configuration between a regular neutral state $\cdots D^0 A^0 \cdots$ and a polar dimerized ionic state $\cdots (D^+ A^-) \cdots$, which has two equivalent configurations with opposite dipole moment, as shown in Fig. 4. One successful example is the tetrathiafulvalene–p-chloranil (TTF–CA) complex, in which electronic and structural changes are coupled, with TTF serving as the electron donor and CA as the acceptor. Using time-resolved XRD, a photoinduced paraelectric-to-ferroelectric phase transition has been observed.[32] The neutral state is made of homogeneous nonpolar chains where molecules of D and A are regularly stacked. Photons excite DA pairs into an ionic state, and the coupling between the relaxed species makes the system switch to a metastable macroscopic ferroelectric state. The transition occurs at a low temperature of 81 K. A similar neutral-to-ionic transition has also been observed in TTF–QBrCl$_3$ complex, which has a quasi-1D structure composed of mixed stacks of a π-electron donor (TTF) and acceptor (QBrCl$_3$), undergoing the first order transition at 70 K.[33] At high temperature the system is nominally neutral with a degree of charge transfer of 0.3, and at low temperature it is ionic with a degree of charge transfer of 0.6. Associated with this neutral-to-ionic transition the symmetry is broken via DA dimerization, resulting in spontaneous polarization, as indicated by the measurement of pyroelectric current and the dielectric anomaly. Further insight was gained in 2012, when the hysteresis loops were recorded for both TTF–CA and TTF–QBrCl$_3$ complexes, yielding a large remnant polarization of 6.3 μC cm^{-2} and 6.7 μC cm^{-2}, respectively, complemented by the measurement of the dielectric anomaly.[34] It was noted that the contribution from molecular dipole moments and ionic polarizations to the observed polarization is negligible, and the major contribution is electronic polarization due to colossal effective Born charges of opposite ions enhanced by strong orbital hybridization. This is certainly worth further investigation and exploration. It was argued that their ferroelectricity is governed by intermolecular charge transfer rather than simple displacement of static point charge on molecules, and in fact, the macroscopic polarization was thought to be antiparallel to the ionic displacement. They thus are considered as rare electronic ferroelectrics.

While TTF–CA and its derivatives show fascinating ferroelectric properties at low temperature, supermolecular networks of charge transfer complexes between a pyromellitic diimide-based acceptor (A) and donors that are derivatives of naphthalene (D2), pyrene (D3) and TTF (D4) have recently been developed, showing good ferroelectricity at room temperature.[35] These polar and switchable systems utilize a structural synergy between a hydrogen-bonded network and a charge transfer complex of donor and acceptor in a mixed stack, which self-assembles into an ordered three-dimensional network, stabilized by four non-covalent bonding interactions, including charge-transfer, hydrogen-bonding, π–π stacking and van der Waals forces. Polarization hysteresis was observed in complexes of A–D2, A–D3 and A–D4 at 300 K with remnant polarizations exceeding 1 μC cm^{-2}. At the low temperature of 7 K, the polarization for complex A–D4 was found to be as large as 55 μC cm^{-2}, the highest among known molecular systems. It also exhibits a large dielectric constant over 400 at room temperature, though no dielectric anomaly was observed throughout the temperature range probed. Such large spontaneous polarization is believed to result from the combination of the charge-transfer process and proton dynamics of orientational, displacive and/or transfer-type mechanisms associated with hydrogen bonds in the intermolecular space within the crystal, and this points to another direction for molecular ferroelectrics.

The second strategy for molecular ferroelectricity is to utilize proton transfer in hydrogen bond, which is involved in early ferroelectrics such as Rochelle salt and KDP, leading to suggestions that hydrogen bonding is necessary for ferroelectricity, which was proven to be incorrect later by perovskite oxides. In KDP, the spontaneous polarization arises mainly from displacement of PO_4^{3-} ions, while collective site-to-site transfer of protons in the O–H···O bonds switches the polarization. It thus shows mixed characteristics of order–disorder and displacive transition. Some recent analogs of KDP ferroelectrics are $[C_6H_7N_2]^+ \cdot ClO_4^-$ (dabcoHClO$_4$) and $[C_6H_7N_2]^+ \cdot BF_4^-$ (dabcoHBF$_4$),[36] both of which contain chains of dacboH$^+$ cations bonded by N–H···N hydrogen bond. At room temperature the acidic hydrogen atoms are ordered in the hydrogen bonds, and dynamic disorder of the ions increases when approaching the Curie temperature. Because of the disorder of protons and anions, the chains lose their polarization. Below T_c, the ordering of the anions and protons breaks the symmetry and results in the spontaneous polarization. The direction of the spontaneous polarization is perpendicular to the chains and to hydrogen bonds, and from the displacements of anion and dabcoH$^+$ cation, the spontaneous polarization of dabcoHBF4 is estimated to be 4.34 μC cm^{-2}, in good agreement with the experimental measurement of 4.6 μC cm^{-2}. This thus suggests that the bistable hydrogen bond is an effective mechanism for molecular ferroelectrics. Indeed, spontaneous polarization as high as 16.5 μC cm^{-2} has been subsequently observed in $[C_6H_{12}N_2H]^+ \cdot ReO_4^-$ (dabcoHReO$_4$),[37] wherein all bistable N–H···N hydrogen bonds are parallel and directed in the same sense, instead of following a zigzag pattern. The spontaneous polarization thus derives from the parallel hydrogen bonds and

aligned polar cations in addition to ionic displacement, resulting in a high spontaneous polarization. In other KDP type of ferroelectrics, the contribution from the proton itself to the spontaneous polarization is minor.

Hydrogen bonding also plays an important role in ferroelectric π-conjugated molecular compounds, consisting of a supramolecular assembly of molecules of hydrogen donor (D) and acceptor (A) using a highly directional nature. For example, phenazine (Phz) molecule was used as the base (A), and chloranilic acid (H$_2$ca) and bromanilic acid (H$_2$ba) were used as the strong dibasic acids (D).[38] In these compounds, proton donors or acceptors reside symmetrically on both sides of the respective molecules to form an infinite supramolecular chain through the intermolecular hydrogen bond, as shown in Fig. 5. The crystal structures of Phz-H$_2$xa are nonpolar at room temperature, and both D and A molecules are located at the center of inversion without any disorder in the atomic positions. This suggests that the ferroelectric transition is displacive instead of order–disorder. Hysteresis measurement at 160 K revealed spontaneous polarization over 1 μC cm^{-2}. According to the crystal structure analysis, the displacement of Phz molecules relative to H$_2$ca is only 0.01 Å along the stacking axis, and thus the calculated spontaneous polarization is only 0.07 μC cm^{-2}, much smaller than the experimental value. The discrepancy was attributed to arise from molecular dipole and delocalized electrons in the crystal through intermolecular interaction, and the strong hydrogen bonding suggests possible tautomerism that transforms the neutral crystal with O–H···N bonds into the ionic state with O···H–N$^+$ bonds and simultaneously changes the π-electron molecular geometry. The approach thus demonstrated a concept of molecular ferroelectrics that constitutes: (i) supramolecular structure by co-crystallization of different molecules; (ii) π-conjugated characteristics; and (iii) strong intermolecular hydrogen bonds.

Recently, cooperative proton tautomerism was also demonstrated in single-component ferroelectric croconic acid, with a room temperature spontaneous polarization as large as 20 μC cm^{-2} measured by both hysteresis loop and pyroelectric current.[3] The molecules are hydrogen bonded into a 2D polar sheet, and each one transfers two hydroxyl protons to the carbonyl groups of adjacent molecules during the polarization reversal. A number of characteristics are worth mentioning. Firstly, the molecule has rather large dipole moment, measured to be 9–10 Debye in dioxane solution, which is close to the density functional theory calculation of 7–7.5 Debye. Secondly, the system has hidden pseudo-centricity in its polar phase, and such a small deviation from paraelectric structure makes polarization reversal much easier, realized through
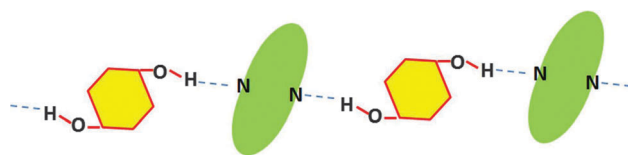

Fig. 5 Schematics of hydrogen bond mechanism in molecular ferroelectrics Phz-H$_2$xa.

the cooperative transformation from O–H···O bond to O···H–O bond and *vice versa* with the simultaneous π-bond switching process. It thus experiences less steric hindrance for polarization reversal than bulk molecular rotation. Nevertheless, no ferroelectric phase transition has been observed. Along similar lines, the β-diketone enol O=C–C=C–H moieties have been explored as a simple prototype for ferroelectric tautomerism.[39] The hydrogen bonding between terminal oxygen atoms links these units in a head-to-tail manner, forming an extended polar molecular chain. The proton transfer therein and the concurrent switching of the π-bond alternation (the keto–enol transformation) can reverse the chain polarity when both occurring cooperatively.[39] By searching for the polar structures with diminished deviation from central-symmetry to ensure easier polarization switching, three single-component ferroelectrics have been discovered, including 2-phenylmalondialdehyde (PhMDA), 3-hydroxyphenalenone (3-HPLN), and cyclobutene-1,2-dicarboxylic acid (CBDC), all having a relatively high Curie temperature around 400 K. These studies established that high-performance ferroelectricity is not specific to croconic acid, and a similar mechanism works in other molecular crystals as well.

By searching the crystal database for polar structures with relatively high melting temperature, exciting molecular ferroelectrics have recently been discovered, including diisopropyl-ammonium chloride (DIPAC) that has a spontaneous polarization of 8.9 μC cm^{-2} and a Curie temperature of 440 K,[40] and diisopropylammonium bromide (DIPAB) that has a spontaneous polarization of 23 μC cm^{-2} and a Curie temperature 426 K.[4,41] The structure phase transition of DIPAB is shown in Fig. 6(a). Comprehensive structure and functional characterizations of these systems have been carried out, which established the ferroelectricity and ferroelectric phase transition convincingly. These include DSC, XRD, and SHG, all confirming structure phase transition at the Curie point, upon which a classical dielectric anomaly was observed that can be fitted by the Curie–Weiss law. The Curie–Weiss constant was found to be 1.32×10^4 K, considerably larger than other molecular ferroelectrics. Away from the phase transition, DIPAB shows a large dielectric constant and a low dielectric loss at room temperature, in addition to its excellent ferroelectric properties. A characteristic lamellar domain pattern has been revealed by PFM, as shown in the amplitude and phase mappings in Fig. 6(b), where the color in the amplitude mapping (left) indicates the magnitude of the piezoresponse, while the two different colors in the phase mapping (right) indicate two domains with opposite polarization directions. The domain walls are evident in the phase mapping, which is also reflected in the amplitude mapping by reduced piezoresponse (blue), across which the polarization direction is different, yet the amplitude is similar. Phase–voltage hysteresis loops and amplitude–voltage butterfly loops were recorded as well, as shown in Fig. 6(c) at three different locations. In addition the $P2_1$ point group symmetry of DIPAB was verified by vertical and lateral PFM as well. The ferroelectricity is believed to arise from the order–disorder behavior of the N atom. When the DIPAB were heated above 426 K, it is observed that the nitrogen atoms enter an apparently disordered state, resulting in a central-symmetric structure.
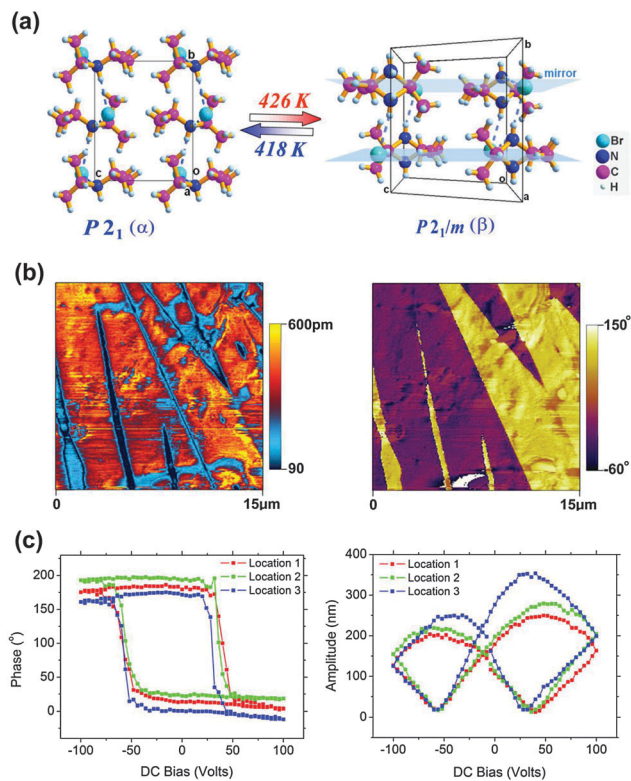
Fig. 6 Ferroelectricity of DIPAB; (a) structure transition; (b) PFM amplitude and phase mappings; and (c) PFM hysteresis and butterfly loops.

First principles calculations suggest that the emergence of the spontaneous polarization in DIPAB is driven by a cooperative atomic distortion that breaks the mirror symmetry plane of each single molecule, resulting in an asymmetric arrangement of the charges. Clearly, DIPAB is a molecular ferroelectric with high spontaneous polarization and Curie temperature that are comparable to BTO, has high dielectric constant and low loss, and exhibits good piezoelectric properties; all these attributes make it a viable molecular alternative to perovskite ferroelectrics.

Finally, we point out that metal organic coordination compound (MOCC) is another promising way to develop molecular ferroelectrics, utilizing the strong and highly directional metal–ligand coordination bonds. This topic has recently been reviewed comprehensively.[31] MOCC bears the advantages of both organic ligands and inorganic ions, with the organic component possessing tailorability, π-conjugation and chirality while the inorganic metal ion possesses hybrid orbital diversity and excellent electronic, magnetic and optical properties. [Co(II)Cl$_3$(H-MPPA)] is one of the successful examples, wherein a 3D framework is created through hydrogen bonds.[42] It has a nice hysteresis loop with spontaneous polarization of 6.8 μC cm^{-2}, and the direction of the spontaneous polarization is perpendicular to the chains and hydrogen bonds. The ferroelectricity of [Co(II)Cl$_3$(H-MPPA)] is thought to arise from bistable hydrogen bonds, similar to that in dabcoHReO$_4$. Much attention has also been focused on MOCC with perovskite-type structure, and Wang and Gao reported [NH$_4$][Zn(HCOO)$_3$],[43] a three-dimensional chiral metal formate
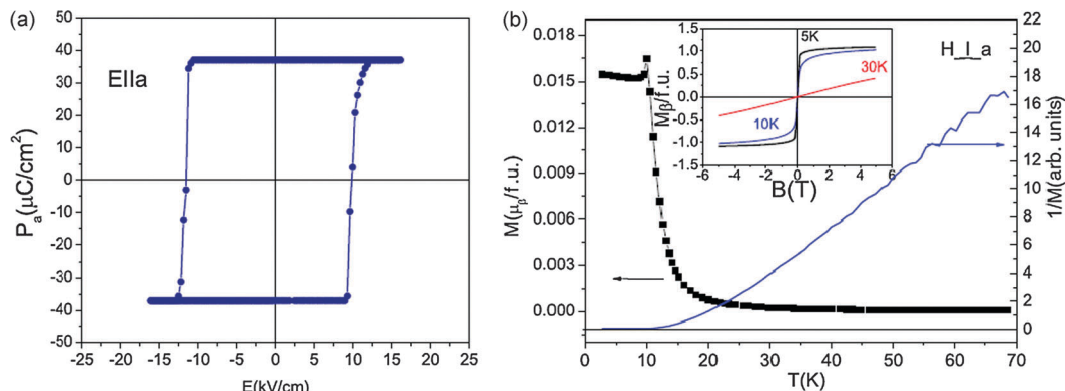
Fig. 7 (a) Ferroelectric hysteresis loop and (b) magnetic transition of [C$_2$H$_5$NH$_3$]$_2$[CuCl$_4$];[44] reprinted with permission from B. Kundys, A. Lappas, M. Viret, V. Kapustianyk, V. Rudyk, S. Semak, C. Simon and I. Bakaimi, *Phys. Rev. B: Condens. Matter Mater. Phys.*, 2010, **81**, 224434. Copyright (2010) by the American Physical Society.

framework compound, which undergoes a paraelectric-to-ferroelectric phase transition at 191 K triggered by the disorder–order transition of NH$_4^+$ cations; a ferroelectric hysteresis loop has been successfully recorded.

Within the group of ferroelectric MOCCs, we note [C$_2$H$_5$NH$_3$]$_2$[CuCl$_4$] as a molecular multiferroic.[44] It possesses a perovskite-type layered structure, and there are infinite layers of corner-sharing Jahn–Teller distorted CuCl$_6$ octahedra with layers of ethylammonium groups attached to each side. The ethylammonium heads form strong hydrogen bonds to all of the eight chloride ions. A dielectric anomaly is found around 247 K, and the phase transition is of the second-order type, with its origin ascribed to the ordering of the organic [C$_2$H$_5$NH$_3$]$^+$. It has a large remnant polarization of 37 μC cm^{-2} at 77 K, as shown in Fig. 7(a), and even more interestingly, it shows ferromagnetic interactions with a magnetic phase transition at T_c of 10.2 K, as shown in Fig. 7(b). This suggests that in such hybrid perovskites, the underlying hydrogen bonding of easily tunable organic building blocks in combination with the 3d transition-metal layers offers an emerging pathway to engineer molecular multiferroics, which opens exciting frontiers in molecular electronics and spintronics.

## 5. Emergence of biological ferroelectricity

In addition to the substantial progresses in molecular ferroelectrics that has been made in the last a few years, exciting developments have also emerged in electromechanical coupling of biological systems. Toward this end, it is first noted that the imidazole unit, which is ubiquitous in biological systems, has recently been explored for molecular ferroelectrics as well. Its proton donor and acceptor moieties easily bind molecules into a dipolar chain, which is often bistable in polarity, and is electrically switchable through proton tautomerization.[45] Indeed, polarization hysteresis loops reveal high spontaneous polarization ranging from 5 to 10 μC cm^{-2}, and such molecular ferroelectrics stand right between electronics and biology, offering numerous opportunities for bio-electric interfaces.

It is well known that many biological tissues are piezoelectric, including bone,[21] teeth,[46] muscles,[47] nerves,[26] exoskeletons,[48]

and otoliths,[49] and piezoelectricity was thought to be a fundamental property of biological tissues.[22] Given the relationship of piezoelectricity and pyroelectricity shown in Fig. 1(a), it is not surprising that pyroelectricity was observed in many biological systems as well.[50] Athensaedt carried out systematic studies of pyroelectricity in both animal and plant tissues from a variety of species,[51] and it was suggested that pyroelectricity might be of fundamental physiological importance to sensory organs.[52] These early development has been documented in a comprehensive review by Lang in 1981.[53] After the discovery of piezoelectricity and pyroelectricity in biological systems, it is only logical to expect biological ferroelectricity as well. Hysteresis loops were indeed recorded in 1960s in NaDNA and RNA, and were attributed to ferroelectricity, though it was later concluded that the phenomenon arises from nonlinear conductivity instead of ferroelectricity.[53] Such an experimental artifact has recently been highlighted by Scott, who demonstrated a hysteresis artifact in banana skin.[54]

Piezoresponse force microscopy (PFM) is a powerful tool to probe electromechanical coupling in piezoelectric and ferroelectric systems at nanoscale,[29,55–57] and in recent years, it has been applied to study a variety of biological materials, including human bones[58] and teeth,[59] tooth dentin and enamel,[60,61] collagen fibrils,[62–64] and insulin and lysozyme amyloid fibrils, breast adenocarcinoma cells, and bacteriorhodopsin.[65] While these studies unambiguously established piezoelectricity in biological systems, biological ferroelectricity remains elusive, and no switching behaviors were observed in a number of systems probed, such as a single collagen.

The first indication of ferroelectricity in biological tissue was reported by Li and Zeng in green abalone shell using PFM,[5] showing typical PFM hysteresis and butterfly loops. They have since carried out PFM studies on clamshell and nacre shell as well, and found consistent switching in these systems.[66–68] Shortly after, we have observed biological ferroelectricity in the aortic wall,[7] and almost simultaneously, ferroelectricity was reported in gamma-glycine as well, the smallest amino acid commonly found in protein.[6] We subsequently showed that ferroelectricity in the aortic wall originates from elastin,[8] as shown in Fig. 8,

(a)

(b)
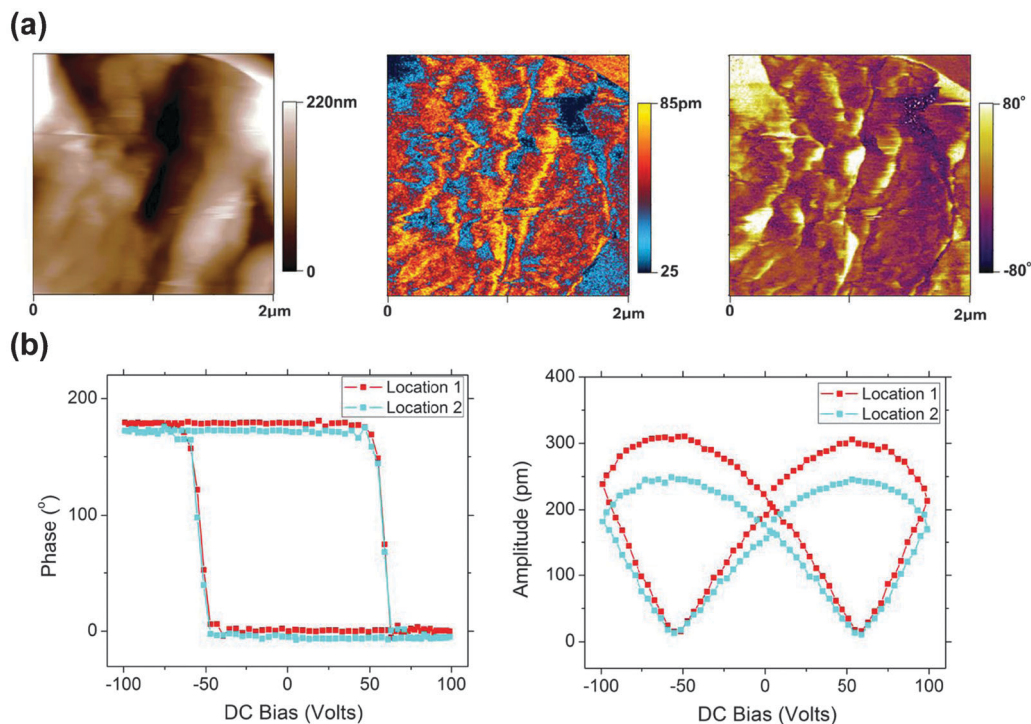
Fig. 8 Ferroelectricity of aortic elastin; (a) mappings of topography, PFM amplitude, and phase; and (b) PFM hysteresis and butterfly loops measured at two different locations.

while collagen was not found to be switchable. It is interesting to note that collagen is a much more ancient protein than elastin, which is only found in the arteries of vertebrate and in later stage of embryonic development, when blood pressure becomes much higher. This suggests that ferroelectric switching may play a role in damping increased pulsatile flow and blood pressure.[69] In addition, pyroelectricity has long been thought to play a fundamental role in the processes of morphogenesis,[70] which correlates well with observations that elastin is a molecular determinant of late arterial morphogenesis.[71] Furthermore, it was discovered that ferroelectric switching in elastin is largely suppressed by glucose, and this could be related to aging, during which glycation between elastin and sugar naturally occurs. Finally, we note that nacre shells are switchable, while bones are not. They have similar inorganic constituents, yet different organic components. Bone contains mostly collagens, while shell contains elastic biopolymers such as chitins, which is closer to elastin in its elasticity. Nevertheless, the 180° contrast of the PFM phase, both in-plane and out-of-plane, have recently been observed in rat tail tendon.[72] Thus it is entirely possible that the required coercive field is too large for switching to be realized in bones and tendons experimentally.

6. Applications and implications

Ferroelectric materials have many important technological applications, and so far the field is dominated by perovskite oxides because of their superior piezoelectric and ferroelectric properties. In the last a few years, a number of new molecular

ferroelectrics have been developed, with ferroelectric properties approaching their inorganic counterparts. These molecular ferroelectrics are soft, flexible, lightweight, environmentally friendly, biocompatible, and can be easily processed at relatively low temperature and printed onto soft substrates. They thus are promising for a wide range of applications including sensing, actuation, energy harvesting, and data storage. With the discoveries of biological ferroelectricity in soft tissues, direct bio-electric interfaces are also possible, opening many more exciting opportunities.

The most widely used molecular ferroelectrics are PVDF based polymers and copolymers,[74] as they have been around for more than 40 years. Much of the recent efforts are devoted toward ferroelectric memories, as recently reviewed,[75] and one interesting application is a banknote integrated with non-volatile organic ferroelectric memory.[76] Flexible programmable logic gates have been developed with ferroelectric multilayers, capable of logical "AND" and "OR" operation.[77] VDF oligomer was also explored for medical use as a new tactile sensor.[78] One distinct advantage of molecular ferroelectrics is that they can be directly printed, as demonstrated in an all-printed ferroelectric active matrix sensor network using P(VDF-TrFE).[79] Recently, energy harvesting that converts mechanical vibration into electricity has also caught much attention, and many interesting concepts have been proposed, including a wearable nanogenerator on the human arm that generates electricity by folding and releasing elbow,[73] as shown in Fig. 9. Other examples include PVDF microbelts for harvesting energy from respiration,[80] and a nanogenerator that is driven by a sonic wave.[81] While all these
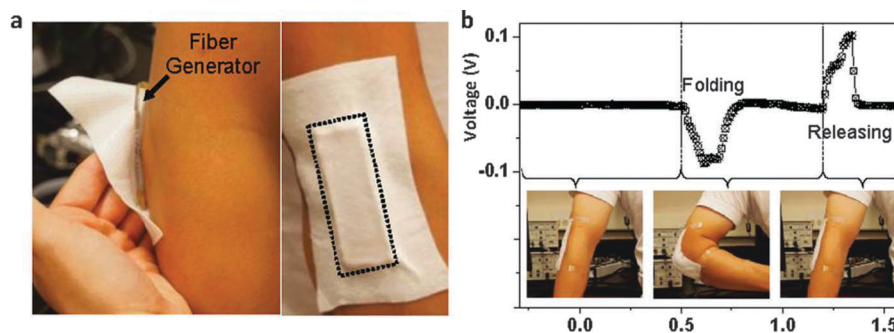
Fig. 9 Wearable nanogenerator attached on an elbow (a), and the voltage produced during folding and releasing of the elbow;[73] reprinted with permission from M. Lee, C.-Y. Chen, S. Wang, S. N. Cha, Y. J. Park, J. M. Kim, L.-J. Chou and Z. L. Wang, *Adv. Mater.*, 2012, **24**, 1759–1764. Copyright © 2012 WILEY-VCH Verlag GmbH & Co. KGaA, Weinheim.

prototype devices are based on PVDF and its copolymers, we expect that newly developed molecular ferroelectrics will enter the field soon, and thus enable many more applications. It is also worth noting that flexible and stretchable PZT ribbons have been developed recently,[82,83] which will enable biomedical applications as well.

Even more exciting are the opportunities offered by biological ferroelectricity, which can interact directly with molecular ferroelectrics. Instead of using molecular ferroelectrics as passive devices in the human body, we can envision future bio-electric interfaces enabled by the ferroelectric effect of the tissues. In particular, it could be possible to monitor the polarization state of biological system for early diagnosis, to manipulate actively the ferroelectric state for repair and mitigation of damage, and to encode information directly into the human body through the polarization states. All of these are purely imaginary at the moment, but with future advances in molecular ferroelectrics and further understanding of biological ferroelectricity, such aspirations may come to life sooner rather than later.

7. Concluding remarks

In the last several years, we have witnessed spectacular advances in both molecular ferroelectrics and biological ferroelectricity. These developments have been made possible by close collaboration across multiple disciplines, and we call for continued collaborations among chemists, physicists, biologists, material scientists and engineers to overcome the many challenges ahead. These include a deep fundamental understanding of the molecular mechanisms of ferroelectricity in general and biological ferroelectricity in particular. Further advances in supramolecular crystal engineering are also desired to enable and facilitate molecular ferroelectrics by design. The physiological and pathological significance of biological ferroelectricity are currently poorly understood, and such understanding would be necessary for bio-electric interfaces that take advantage of these effects. We believe molecular ferroelectrics represent an exciting frontier between electronics and biology, and we anticipate many more exciting discoveries and developments in the years to come.

References

1 J. F. Nye, *Physical Properties of Crystals*, Oxford, Clarendon Press, 1957.
2 M. E. Lines and A. M. Glass, *Principles and Applications of Ferroelectrics and Related Materials*, Oxford University Press, 1977.
3 S. Horiuchi, Y. Tokunaga, G. Giovannetti, S. Picozzi, H. Itoh, R. Shimano, R. Kumai and Y. Tokura, *Nature*, 2010, **463**, 789–792.
4 D. W. Fu, H. L. Cai, Y. M. Liu, Q. Ye, W. Zhang, Y. Zhang, X. Y. Chen, G. Giovannetti, M. Capone, J. Y. Li and R. G. Xiong, *Science*, 2013, **339**, 425–428.
5 T. Li and K. Zeng, *Acta Mater.*, 2011, **59**, 3667–3679.
6 A. Heredia, V. Meunier, I. K. Bdikin, J. Gracio, N. Balke, S. Jesse, A. Tselev, P. K. Agarwal, B. G. Sumpter, S. V. Kalinin and A. L. Kholkin, *Adv. Funct. Mater.*, 2012, **22**, 2996–3003.
7 Y. Liu, Y. Zhang, M. Chow, Q. N. Chen and J. Li, *Phys. Rev. Lett.*, 2012, **108**, 078103.
8 Y. Liu, Y. Wang, M. Chow, N. Q. Chen, F. Ma, Y. Zhang and J. Li, *Phys. Rev. Lett.*, 2013, **110**, 168101.
9 J. Curie and P. Curie, *C. R. Acad. Sci. Paris*, 1880, **91**, 294–297.
10 J. Valasek, *Phys. Rev.*, 1921, **17**, 475–481.
11 G. Busch and P. Scherrer, *Naturwissenschaften*, 1935, **23**, 737–738.
12 A. von Hippel, R. G. Breckenridge, F. G. Chesley and L. Tisza, *Ind. Eng. Chem.*, 1946, **38**, 1097–1109.
13 G. Shirane and A. Takeda, *J. Phys. Soc. Jpn.*, 1952, **7**, 5–11.
14 E. Sawaguchi, *J. Phys. Soc. Jpn.*, 1953, **8**, 615–629.
15 H. Kawai, *Jpn. J. Appl. Phys.*, 1969, **8**, 975–976.

16 J. G. Bergman, J. H. McFee and G. R. Crane, *Appl. Phys. Lett.*, 1971, **18**, 203–205.

17 R. G. Kepler and R. A. Anderson, *J. Appl. Phys.*, 1978, **49**, 1232–1235.

18 A. J. P. Martin, *Proc. Phys. Soc.*, 1941, **53**, 186–189.

19 V. A. Bazhenov and V. A. Konstantinova, *Dokl. Akad. Nauk SSSR*, 1950, **71**, 283; V. A. Bazhenov and V. A. Konstantinova, *Chem. Abstr.*, 1951, **45**, 2747.

20 V. A. Bazhenov, *Dokl. Akad. Nauk SSSR*, 1953, **90**, 281.

21 E. Fukada and I. Yasuda, *J. Phys. Soc. Jpn.*, 1957, **12**, 1158–1162.

22 M. H. Shamos and L. S. Lavine, *Nature*, 1967, **213**, 267–269.

23 L. R. Duarte, *Arch. Orthop. Trauma. Surg.*, 1983, **101**, 153–159.

24 S. B. Lang, *Nature*, 1966, **212**, 704.

25 H. Athensta, *Ann. N. Y. Acad. Sci.*, 1974, **238**, 68–94.

26 S. B. Lang, *IEEE Trans. Dielectr. Electr. Insul.*, 2000, **7**, 466–473.

27 H. R. Leuchtag and V. S. Bystrov, *Ferroelectrics*, 1999, **220**, 157–204.

28 H. L. Cai, W. Zhang, J. Z. Ge, Y. Zhang, K. Awaga, T. Nakamura and R. G. Xiong, *Phys. Rev. Lett.*, 2011, **107**, 147601.

29 S. V. Kalinin, B. J. Rodriguez, S. Jesse, E. Karapetian, B. Mirman, E. A. Eliseev and A. N. Morozovska, *in Annual Review of Materials Research*, Annual Reviews, Palo Alto, 2007, vol. 37, pp. 189–238.

30 S. Horiuchi and Y. Tokura, *Nat. Mater.*, 2008, **7**, 357–366.

31 W. Zhang and R. G. Xiong, *Chem. Rev.*, 2012, **112**, 1163–1195.

32 E. Collet, M. H. Lemee-Cailleau, M. Buron-Le Cointe, H. Cailleau, M. Wulff, T. Luty, S. Y. Koshihara, M. Meyer, L. Toupet, P. Rabiller and S. Techert, *Science*, 2003, **300**, 612–615.

33 F. Kagawa, S. Horiuchi, H. Matsui, R. Kumai, Y. Onose, T. Hasegawa and Y. Tokura, *Phys. Rev. Lett.*, 2010, **104**, 227602.

34 K. Kobayashi, S. Horiuchi, R. Kumai, F. Kagawa, Y. Murakami and Y. Tokura, *Phys. Rev. Lett.*, 2012, **108**, 237601.

35 A. S. Tayi, A. K. Shveyd, A. C. H. Sue, J. M. Szarko, B. S. Rolczynski, D. Cao, T. J. Kennedy, A. A. Sarjeant, C. L. Stern, W. F. Paxton, W. Wu, S. K. Dey, A. C. Fahrenbach, J. R. Guest, H. Mohseni, L. X. Chen, K. L. Wang, J. F. Stoddart and S. I. Stupp, *Nature*, 2012, **488**, 485–489.

36 A. Katrusiak and M. Szafranski, *Phys. Rev. Lett.*, 1999, **82**, 576–579.

37 M. Szafranski, A. Katrusiak and G. J. McIntyre, *Phys. Rev. Lett.*, 2002, **89**, 215507.

38 S. Horiuchi, F. Ishii, R. Kumai, Y. Okimoto, H. Tachibana, N. Nagaosa and Y. Tokura, *Nat. Mater.*, 2005, **4**, 163–166.

39 S. Horiuchi, R. Kumai and Y. Tokura, *Adv. Mater.*, 2011, **23**, 2098–2103.

40 D. W. Fu, W. Zhang, H. L. Cai, J. Z. Ge, Y. Zhang and R. G. Xiong, *Adv. Mater.*, 2011, **23**, 5658–5662.

41 A. Piecha, A. Gagor, R. Jakubas and P. Szklarz, *CrystEngComm*, 2013, **15**, 940–944.

42 H. Y. Ye, D. W. Fu, Y. Zhang, W. Zhang, R. G. Xiong and S. D. Huang, *J. Am. Chem. Soc.*, 2009, **131**, 42–43.

43 G. C. Xu, X. M. Ma, L. Zhang, Z. M. Wang and S. Gao, *J. Am. Chem. Soc.*, 2010, **132**, 9588–9590.

44 B. Kundys, A. Lappas, M. Viret, V. Kapustianyk, V. Rudyk, S. Semak, C. Simon and I. Bakaimi, *Phys. Rev. B: Condens. Matter Mater. Phys.*, 2010, **81**, 224434.

45 S. Horiuchi, F. Kagawa, K. Hatahara, K. Kobayashi, R. Kumai, Y. Murakami and Y. Tokura, *Nat. Commun.*, 2012, **3**, 1308.

46 H. Athenstaedt, *Arch. Oral Biol.*, 1971, **16**, 495–501.

47 E. Fukada and H. Ueda, *Jpn. J. Appl. Phys.*, 1970, **9**, 844–845.

48 R. M. Zilberst, *Nature*, 1972, **235**, 174–175.

49 R. W. Morris and L. R. Kittlema, *Science*, 1967, **158**, 368–370.

50 S. B. Lang, *Nature*, 1966, **212**, 704–705.

51 H. Athenstaedt, *Ann. N. Y. Acad. Sci.*, 1974, **238**, 68–94.

52 H. Athenstaedt, H. Claussen and D. Schaper, *Science*, 1982, **216**, 1018–1020.

53 S. B. Lang, *Ferroelectrics*, 1981, **34**, 257–263.

54 J. F. Scott, *J. Phys.: Condens. Matter*, 2008, **20**, 021001.

55 A. Gruverman and S. V. Kalinin, *J. Mater. Sci.*, 2006, **41**, 107–116.

56 S. V. Kalinin, A. Rar and S. Jesse, *IEEE Trans. Ultrason. Ferroelectr. Freq. Control*, 2006, **53**, 2226–2252.

57 D. A. Bonnell, S. V. Kalinin, A. L. Kholkin and A. Gruverman, *MRS Bull.*, 2009, **34**, 648–657.

58 C. Halperin, S. Mutchnik, A. Agronin, M. Molotskii, P. Urenski, M. Salai and G. Rosenman, *Nano Lett.*, 2004, **4**, 1253–1256.

59 A. Gruverman, D. Wu, B. J. Rodriguez, S. V. Kalinin and S. Habelitz, *Biochem. Biophys. Res. Commun.*, 2007, **352**, 142–146.

60 S. V. Kalinin, B. J. Rodriguez, S. Jesse, T. Thundat and A. Gruverman, *Appl. Phys. Lett.*, 2005, **87**, 053901.

61 B. J. Rodriguez, S. V. Kalinin, J. Shin, S. Jesse, V. Grichko, T. Thundat, A. P. Baddorf and A. Gruverman, *J. Struct. Biol.*, 2006, **153**, 151–159.

62 M. Minary-Jolandan and M.-F. Yu, *ACS Nano*, 2009, **3**, 1859–1863.

63 M. Minary-Jolandan and M. F. Yu, *Nanotechnology*, 2009, **20**, 085706.

64 C. Harnagea, M. Vallieres, C. P. Pfeffer, D. Wu, B. R. Olsen, A. Pignolet, F. Legare and A. Gruverman, *Biophys. J.*, 2010, **98**, 3070–3077.

65 S. V. Kalinin, B. J. Rodriguez, S. Jesse, K. Seal, R. Proksch, S. Hohlbauch, I. Revenko, G. L. Thompson and A. A. Vertegel, *Nanotechnology*, 2007, **18**, 424020.

66 T. Li and K. Y. Zeng, *J. Struct. Biol.*, 2012, **180**, 73–83.

67 T. Li, L. Chen and K. Y. Zeng, *Acta Biomater.*, 2013, **9**, 5903–5912.

68 T. Li and K. Zeng, *J. Appl. Phys.*, 2013, **113**, 187202.

69 B. Chen and H. Gao, *Phys. J.*, 2012, **5**, 19.

70 H. Athenstaedt, *Ann. N. Y. Acad. Sci.*, 1974, **238**, 68–94.

71 D. Y. Li, B. Brooke, E. C. Davis, R. P. Mecham, L. K. Sorensen, B. B. Boak, E. Eichwald and M. T. Keating, *Nature*, 1998, **393**, 276–280.

72 D. Denning, M. T. Abu-Rub, D. I. Zeugolis, S. Habelitz, A. Pandit, A. Fertala and B. J. Rodriguez, *Acta Biomater.*, 2012, **8**, 3073–3079.

73 M. Lee, C. Y. Chen, S. Wang, S. N. Cha, Y. J. Park, J. M. Kim, L. J. Chou and Z. L. Wang, *Adv. Mater.*, 2012, **24**, 1759–1764.

74 *Ferroelectric Polymers: Chemistry, Physics, and Applications*, ed. H. S. Nalwa, CRC Press, 1995.

75 K. Asadi, M. Y. Li, P. W. M. Blom, M. Kemerink and D. M. de Leeuw, *Mater. Today*, 2011, **14**, 592–599.

76 M. A. Khan, U. S. Bhansali and H. N. Alshareef, *Adv. Mater.*, 2012, **24**, 2165–2170.

77 S. Horie, K. Noda, H. Yamada, K. Matsushige, K. Ishida and S. Kuwajima, *Appl. Phys. Lett.*, 2007, **91**, 193506.

78 K. Takashima, S. Horie, T. Mukai, K. Ishida and K. Matsushige, *Sens. Actuators, A*, 2008, **144**, 90–96.

79 M. Zirkl, A. Sawatdee, U. Helbig, M. Krause, G. Scheipl, E. Kraker, P. A. Ersman, D. Nilsson, D. Platt, P. Bodo, S. Bauer, G. Domann and B. Stadlober, *Adv. Mater.*, 2011, **23**, 2069–2074.

80 C. L. Sun, J. Shi, D. J. Bayerl and X. D. Wang, *Energy Environ. Sci.*, 2011, **4**, 4508–4512.

81 S. Cha, S. M. Kim, H. Kim, J. Ku, J. I. Sohn, Y. J. Park, B. G. Song, M. H. Jung, E. K. Lee, B. L. Choi, J. J. Park, Z. L. Wang, J. M. Kim and K. Kim, *Nano Lett.*, 2011, **11**, 5142–5147.

82 Y. Qi, J. Kim, T. D. Nguyen, B. Lisko, P. K. Purohit and M. C. McAlpine, *Nano Lett.*, 2011, **11**, 1331–1336.

83 X. Feng, B. D. Yang, Y. Liu, Y. Wang, C. Dagdeviren, Z. Liu, A. Carlson, J. Li, Y. Huang and J. A. Rogers, *ACS Nano*, 2011, **5**, 3326–3332.